-RESEARCH PAPER-

International Journal of Mining and Geo-Engineering

IJMGE

IJMGE 56-4-(2022) 401-411

DOI: 10.22059/IJMGE.2022.339174.594951

Development of new comprehensive relations to assess rock fragmentation by blasting for different open-pit mines using GEP algorithm and MLR procedure

Hassan Moomivand [a], Hasel Amini Khoshalan [b,*], Jamshid Shakeri [b], Hassan Vandyousefi [a]

[a] *Mining Engineering Department, Urmia University, Urmia, Iran.*

[b] *Mining Engineering Department, Engineering Faculty, University of Kurdistan, Sanandaj, Iran.*

Article History:

Received: 14 February 2022.

Revised: 16 May 2022.

Accepted: 17 June 2022.

ABSTRACT

The fragment size of blasted rocks considerably affects the mining costs and production efficiency. The larger amount of blasthole diameter (ϕ_h) indicates the larger blasting pattern parameters, such as spacing (S), burden (B), stemming (S_t), charge length (L_e), bench height (K), and the larger the fragment size. In this study, the influence of blasthole diameter, blastability index (BI), and powder factor (q) on the fragment size were investigated. First, the relation between each of X_{20}, X_{50}, and X_{80} with BI, ϕ_h, and q as the main critical parameters were analyzed by Table curve v.5.0 software to find better input variables with linear and nonlinear forms. Then, the results were analyzed by multivariable linear regression (MLR) procedure using SPSS v.25 software and gene expression programming (GEP) algorithm for prepared datasets of four open-pit mines in Iran. Relations between each of X_{20}, X_{50}, and X_{80} with the combination of adjusted BI, ϕ_h, and q were obtained by MLR procedure with good correlations of determination (R^2) and less root mean square error (RMSE) values of (0.811, 1.4 cm), (0.874, 2.5 cm) and (0.832, 5.4 cm) respectively. Moreover, new models were developed to predict X_{20}, X_{50}, and X_{80} by the GEP algorithm with better correlations of R^2 and RMSE values (0.860, 1.3 cm), (0.913, 2.49 cm), and (0.885, 5.6 cm) respectively and good agreement with actual field results. The developed GEP models can be used as new relations to estimate the fragment sizes of blasted rocks.

Keywords: *Rock fragmentation, Blasting, Open-pit mines, Multivariable linear regression, Gene expression programming.*

1. Introduction

Despite the development of advanced rock cutting and excavation machines, nowadays drilling and blasting as an important flexible method is applied for excavating hard rock and different rock mass conditions in mining and civil engineering projects. Blasting operations are used for rock fragmentation and displacement in which only around 15 to 20 percent of the transmitted explosive energy is utilized and improper utilization of energy not only leads to improper larger fragments but also results in side effects such as more ground vibrations, flyrock, etc. [1-7]. The degree of rock fragmentation and fragment size distribution can also be different for special applications [8]. Rock fragment size needs to be suitable for loading and without a high percentage of large boulders. On the other hand, fine fragments lead to high consuming energy and dust pollution. The cost of loading, haulage, and rock crushing decreases with an increase in rock fragmentation, whereas drilling and blasting costs increase [9]. For these reasons, the fragment size is a more significant result of blasting operations.

The fragment size of blasted rocks mainly depends on some in-situ rock mass properties and blasthole parameters. Due to the complexity of effective parameters on the rock fragmentation results, accurate prediction of fragment size distribution has long been an important problem in blasting operations. Different methods have been presented to evaluate the fragment size in blasting operations including empirical methods [10-12], artificial intelligence algorithms [13-16], rock engineering systems [17,18], and multivariate analytical methods [19]. Rock mass properties, blasting pattern parameters, and powder factor significantly vary from one mine to another. The fragment size distribution results can also vary from one zone to another in different mines. For the development of comprehensive relations to assess rock fragmentation by blasting operation in open-pit mines, data with wide ranges of rock mass properties, powder factor, and blasting pattern parameters are necessary. For using the results of one mine with one blasthole diameter (ϕ_h), there is not a very wide variation in rock mass properties and the blasthole diameter as a critical parameter that represents the scale factor in drilling and blasting has a constant value. The larger amount of ϕ_h generally indicates the larger blasting pattern, such as spacing, burden, stemming length, blasthole depth, and the larger the fragments. On the other hand, a powerful method is needed to analyze different types of inhomogeneous data to achieve reliable models. Empirical models such as Kuznetsov's model, Kuz-Ram model, and modified Kuz – Ram model have widely been used for the assessment of rock fragmentation in blasting operations. Due to the complexity of the affecting parameters on the fragmentation results of blasted rocks, as well as detailed knowledge of geo-mechanical conditions, the performance of these models is not more acceptable in different surface mining blasting (e.g. 32.6 to 39.9% error has been reported) [20].

Because of the high ability of artificial intelligence algorithms and multivariate analytical procedures in analyzing complex problems, these

* Corresponding author: *E-mail address:* h.amini@uok.ac.ir (H. Amini Khoshalan).

techniques have been used to improve the problems in several fields of mining engineering especially rock fragmentation [21-35].

Monjezi et al. [36] used Fuzzy logic (FL) for predicting the size of fragmented rocks in the Golgohar iron ore open-pit mine. They used parameters of spacing (S), burden (B), specific drilling (SD), blasthole depth (L), stemming length (S_t), the charge per delay (Ch), rock density (RD), and powder factor (q) as input parameters. The results showed that fuzzy logic has a high ability to predict rock fragmentation. Ebrahimi et al. [37] applied artificial neural networks (ANNs) and ant bee colony (ABC) algorithm for the prediction and optimization of rock fragmentation and backbreak in Anguran lead and zinc open-pit mine, and B, S, S_t, L, and q were used as input parameters. In another study, for predicting rock fragmentation and flyrock in the Tajareh limestone mine, the ANN technique and firefly algorithm (FAA) were implemented considering B, S, L, SD, Ch, q, and geological strength index (GSI) as input parameters by Faraji asl et al. [38]. Hassanipanah et al. [28] investigated the feasibility of the PSO*-ANFIS† model for the prediction of rock fragmentation (X_{80}) using B, S, St, q, and Ch as input parameters and compared the results with SVM‡ and NMR∫ methods. Their results presented the high capability of the PSO-ANFIS model in predicting rock fragmentation. The relation between blast parameters (B, S, St, L, q, and Ch) and rock size distribution (RSD) was performed using a combination of different AI techniques such as ant colony optimization - boosted regression tree (ACO - BRT), FFA– ANN and PSO – ANFIS by Zhang et al. [15] in a limestone mine in Vietnam. According to their results, the ACO-BRT model revealed more accuracy than other methods. Cat swarm optimization (CSO) as another sub-branch of AI and the PSO methods were applied to predict the rock fragment size (X_{80}) as a function of the blast parameters (B, S, St, q, Ch) and RMR by Huang et al. [39]. A comparison of the results showed that the CSO has higher accuracy than the PSO model in predicting rock fragmentation. Fang et al. [29] predicted blast-induced rock fragmentation in a limestone quarry in Vietnam by SVM, FFA-ANN, FFA-BGAM, Gaussian process regression, and k-nearest neighbors (KNN) methods. In this study, the inputs were the same as the inputs of the most reported studies in the field of predicting rock fragmentation including controllable blast parameters (bench height, q, Ch, St, B, and S). The results presented that the FFA-BGAM method has the highest correlation of determination (R^2) and lowest root mean square error (RMSE) and mean absolute error (MAE).

Most previous studies on the evaluation and prediction of rock fragment sizes such as X_{50} or X_{80} have been carried out based on the blast data in one mine. Hence, the presented models are reliable for the conditions in which the studies have been performed and cannot be generalized to further open-pit mines. Moreover, the user input parameters in most of the studies are more or less similar and include the controllable blast pattern parameters and less attention has been paid to using the blastability index (BI) as representative of the effects of important parameters on rock fragmentation including uniaxial compressive strength (UCS), rock mass description, joint plane orientation, joint plane spacing a Specific gravity influence parameters. On the other hand, most of the used controllable blast parameters such as bench height, spacing, burden, stemming, blasthole depth, and sub–drilling considered as input parameters in these mentioned studies, have a directly and closely related to the blasthole diameter that have parallel effects the same as blasthole diameter on rock fragments size. Hence, for the first time, these parallel parameters have not been considered in this study, and effective parameters including blasthole diameter, powder factor, and BI were applied as input parameters for evaluation and prediction of blast-induced rock fragmentation (X_{20}, X_{50}, and X_{80}). X_{20}, X_{50}, and X_{80} are the important fragment sizes of blasted rocks as X_{80} - X_{50} = X_{50} – X_{20} =30 and uniformity index (n) of fragment size distribution curve in Rosin-Rammler [43] equation is determined by X_{50} and X_{80}, [n = 0.842 / (ln X_{80} – ln X_{50})] or X_{20} and X_{50}, [n=1.133 / (ln X_{50} – ln X_{20}]. For this purpose, 53 datasets from different zones of four open-pit mines were prepared to achieve comprehensive and new relations for the evaluation of rock fragmentation by MLR procedure and GEP algorithm.

2. Methodology

2.1. Multivariable linear regression procedure

Multivariable linear regression (MLR), a common procedure in multivariate analysis, is based on a linear relationship between input or independent variables and the output or dependent variable. If a linear relationship is recognized between a dependent variable and an independent variable, the regression technique is called simple linear regression. However, if several descriptive or independent variables are used for analysis, the regression analysis is called multivariable linear regression [40, 44]. In this study, the dependent variable is each fragment size (X_{20}, X_{50}, and X_{80}), and the independent variables are ϕ_h, q, and BI. The larger amount of blasthole diameter (ϕ_h) indicates the larger blasting pattern parameters, such as spacing (S), burden (B), stemming (S_t), charge length (L_e), bench height (K), and the larger the fragment size. Therefore, blasthole diameter represents the role of S, B, S_t, L_e, and K on the fragment sizes of blasted rocks. BI also represents the influence of five rock mass parameters on rock fragment sizes including rock mass description (RMD), joint plane spacing (JPS), joint plane orientation (JPO), specific gravity influence (SGI), and uniaxial compressive strength (UCS). The powder factor (q) is an important parameter affecting the rock fragment size.

In multivariable linear regression, estimation of the parameters of a linear model is complete by an objective function and variables values. In linear regression, the model is a linear relation in terms of model parameters. Thus, if we have n observations of the independent variable p next to X and want to establish a linear relationship with the response variable Y, we can use the following linear regression model.

$$Y_i = \beta_0 1 + \beta_1 X_{i1} + \cdots + \beta_p X_{ip} + \varepsilon_i \qquad i = 1,2,\ldots,n \tag{1}$$

Since the independent variable X has a p dimension, its values in each dimension are replaced with an independent variable. It is clear that the index also indicates the observation number and ε is considered the error of the regression model [45].

2.2. Gene Expression Programming

Gene expression programming (GEP) developed by Ferreira in 1999 as a genetic programming technique (GP), is able to generate nonlinear prediction models [46]. This method has been used for solving a multitude of complex engineering problems [47-53]. GEP is based on linear chromosomes with fixed lengths and the structure is composed of trees of different shapes and sizes [54].

The main procedure of the GEP algorithm is shown in Figure 1. As can be seen, after preparing appropriate datasets, 75% of these data are randomly selected for training process. Then, the initial population process is produced composed of random chromosomes including gen/gens of equal size (known as initial individuals). These chromosomes are coded as tree expressions (ETS) and the fitness of individuals is assessed. Individuals are then selected according to their merits based on the considered evaluation function to be rebuilt with modifications and improvements, leaving children with new characteristics. The termination criterion of this cycle is based on the determined generation's number for achieving the best solution [55-57].

* Particle swarm optimization
† Adaptive neuro fuzzy inference system
‡ Support vector machines
∫ Nonlinear multiple regression

It should be noted that reproduction involves the activity of genetic operators with the capability of producing genetic diversity. Reproduction involves duplication and genetic modification. Duplication is an operation that keeps several suitable individuals of the present generation for the next generation. Also through the activity of other operators, genetic changes within the population are performed. The chromosomes are randomly selected for modification by operators; thus, in GEP, one chromosome at a time may be modified or not modified at all by one or more genetic operators [58, 59]. It is notable to say that, the information of chromosomes is encoded by the Karva language which is expressed as trees and linear chromosome components include terminals (A, B, C, ...) and functions (+, -, ...).

In the GEP algorithm, constant values are also the main component in the production of chromosomes and are part of the final set. The length of chromosomes and genes in the GEP algorithm is constant and only changes can be observed during the open reading frame (ORF). This causes incompatibility at the GEP endpoint with the gene endpoint, due to the presence of non-coding regions at the end of the gene. These non-coding regions in GEP allow operators to work without restrictions, which creates genetic diversity and is one way of achieving evolution [5].

Genes are made up of two parts, the head (h) and the tail (t), each of which has different functions. The head section is used to encode the functions, and the tail section is the location for the terminals to ensure the formation of a valid structure (Eq 2). Also, the number of variables that the function needs to work is called the number of arguments to the function. For example, the log (x) function has one argument, and the if (x, y) function has two arguments [5,45]. To draw the expression tree, there are rules, which are followed by a hypothetical example (Figure 2) to understand these rules:

$$t = h(n-1) + 1 \quad (2)$$

1. Read the root of the expression tree at the top of the tree.
2. The number of output nodes is determined depending on the root.
3. After the root, the existing functions are given and their output nodes are determined.
4. The number of nodes in the next row is equal to the sum of the current row arguments.
5. Nodes from left to right are filled in the same way as the members of the gene in each row.
6. This process continues until there is finally only one terminal [5,45].

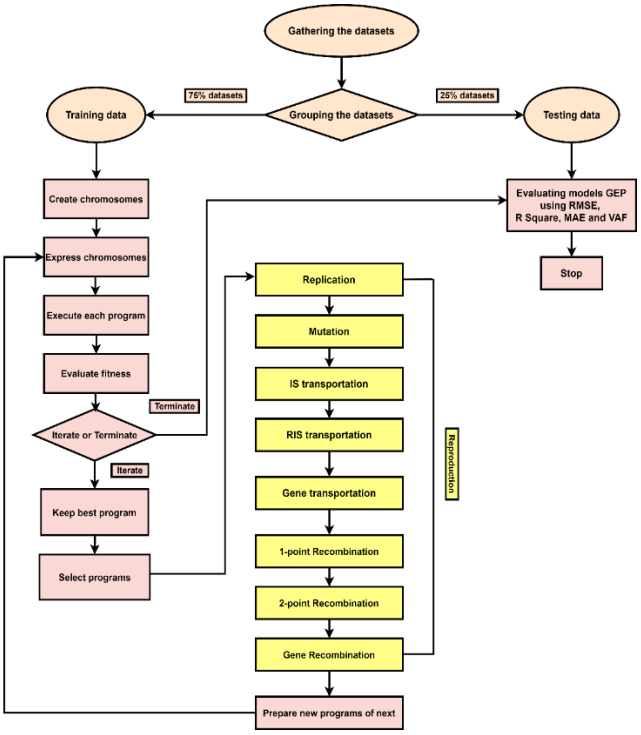

Figure 1. Schematic flowchart of GEP [5,41].

3. Data sets

Rock mass properties, powder factor, and blast pattern parameters are usually varied from one mine to another. Parameters of blast pattern such as spacing (S), burden (B), stemming (S_t), charge length (L_e), and bench height (K) have a good correlation with ϕ_h as they increase with increasing ϕ_h for results of 53 datasets in studied zones of four open-pit mines in Iran including Sungun copper mine, Golgohar iron mine, Soufian, and Rashakan limestone mines (Figure 3). Therefore, blasthole diameter can represent the impacts of the other blasthole parameters on rock fragmentation.

Lilly [60,61] developed the blastability index (BI) as a combination of uniaxial compressive strength (UCS), rock mass description (RMD), specific gravity influence (SGI), joint plane spacing (JPS), and joint plane orientation (JPO) affecting rock fragmentation by blasting as follows:

$$BI = 0.5\,(0.05UCS + RMD + SGI + JPS + JPO) \quad (3)$$

JPS has an important effect on the fragment size, nevertheless, it's rating for a wide range of JPS between 0.1 and 1 m in the evaluation of the BI has a constant value equal to 20, while the most joints spacing is formed in this range, so for highlighting the role of this parameter it is proposed to be adjusted as 20, 30, and 40 for the ranges of 0.1 – 0.2, 0.2–0.5, and 0.5–1.0 m respectively [21]. Therefore, the adjusted values of blastability index were applied (Table 1) and these adjusted BI, blasthole diameter (ϕ_h), and powder factor (q) were considered as the critical effective parameters on the fragment size of blasted rocks in this study. To have a comprehensive dataset for analysis of the blast-induced rock fragmentation, studies were performed in the four mentioned mines as case studies.

Other parts of the datasets are the size of fragmented rocks caused by blasting X_{20}, X_{50}, and X_{80}. These values were measured by the digital image analysis method for the studied zones. In order to determine the distribution of fragmented rock sizes, digital image processing is done by Split Desktop software (version 3.1).[62]. After choosing an image of fragmented rocks in order to define the boundaries of the fragments in the selected image, the methods of automatic or manual can be applied. According to previous studies difference between the Split Desktop results by manual delineation and sieve analysis is less than 3.59% [63, 64]. The process of digital image analysis for a sample of the prepared images in the Rashakan limestone 8-3 zone has been presented in Figure 4. The fragment sizes X_{20}, X_{50} and X_{80} are obtained for each blasting pattern in the studied mines. The input and output parameters, their respective symbols as well as minimum, maximum, and standard deviation values are given in Table 2. The frequency histograms of considered inputs are illustrated in Figure 5.

4. Prediction X_{20}, X_{50}, and X_{80} by statistical models using MLR procedure

Statistical analysis using the MLR procedure is linear. A better correlation between output and input data may be nonlinear multivariable or mixed linear and nonlinear multivariable. First, the interrelation between inputs and outputs were analyzed by Table curve v.5.0 software which has the ability to find better input variables with linear and nonlinear forms and gives the opportunity for better prediction by statistical analysis using MLR procedure. After finding relations between each output data X_{20}, X_{50}, and X_{80} with input data, each relation was used as an independent variable in MLR analysis. Indeed multivariable nonlinear regression is performed by MLR procedure. SPSS v.25 software based on MLR analysis using the backward method was applied to find the best mathematical relations between each of X_{20}, X_{50}, and X_{80} and a combination of BI, ϕ_h, and q variables. In this method, all independent variables are put in the

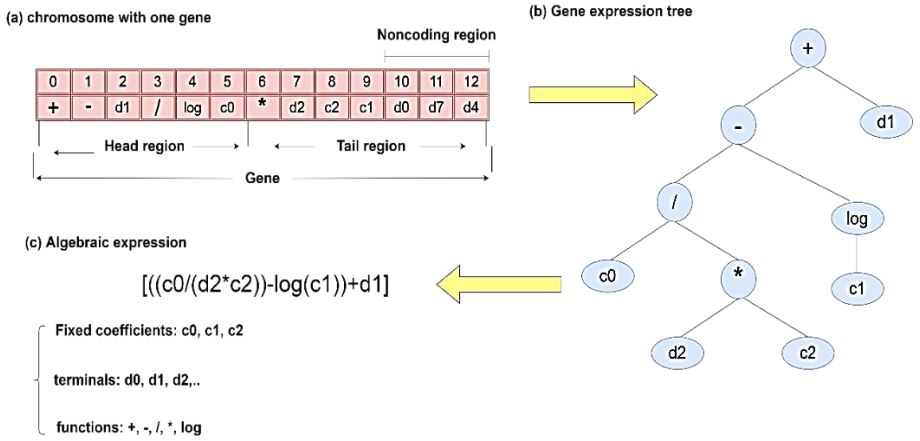

Figure 2. (a) Information of chromosomes by Karva language, (b) expression tree, (c) attained relation.

model at the savariable. Based on previous studies, the performance of each model is evaluated based on RMSE, MAE, $R^{2,}$ and Variance Accounted for (VAF) [65, 66].

$$RMSE = \sqrt{\frac{\sum_{i=1}^{N}(X_{i-Predicted} - X_{i-Measured})^2}{N}} \quad (4)$$

$$MAE = \frac{\sum_{i=1}^{N}| X_{i-Predicted} - X_{i-Measured}|}{N} \quad (5)$$

The parameters of R^2 and VAF are also calculated as follows:

$$R^2 = 1 - \frac{\sum_{i=1}^{N}(X_{i-Predicted} - X_{i-Measured})^2}{\sum_{i=1}^{N}(X_{Mean-Measured} - X_{i-Measured})^2} \quad (6)$$

$$VAF = \left(1 - \frac{VAR(X_{Predicted} - X_{Measured})}{VAR(X_{Measured})}\right) \quad (7)$$

The VAF is considered to verify the correctness of an equation or model so that the value of 1 or 100% displays the best performance. Table 3 displays the best-achieved performance indicators of MLR for predicting rock fragmentation and associated relations between X_{20}, $X_{50,}$ and $X_{80,}$ and a combination of BI, $\phi_{h,}$ and q were obtained (Eqs. 8, 9, and 10).

$$X_{20} = 31.968 - (1.515Ln(\varphi_h^2) - \frac{606.28}{\varphi_h} + 0.105\varphi_h - 4.4667q^2Ln(q) + \frac{1.363}{q} + 0.005BI^{1.5} - \frac{301.383}{BI} \quad (8)$$

$$X_{50} = -186.03674 + 31.733Ln(\varphi_h) + 711.64\frac{Ln(\varphi_h)}{\varphi_h} + 4.4657(Ln(q))^2 - 9.164q^2Ln(q) + 0.317BI \quad (9)$$

$$X_{80} = -81.1977 + 30.355(Ln(\varphi_h))^2 - 29.764(Ln(q))^2 + \frac{0.4998}{Ln(q)} - 0.0052BI^2 - 3238.392BI^{1.5} + 0.8467BI \quad (10)$$

5. Prediction X_{20}, $X_{50,}$ and X_{80} using GEP algorithm

To predict rock fragmentation by GEP algorithm, GeneXproTools 5.0 a powerful software package with an evolutionary computation was applied. Modeling with GEP includes five steps as follows:

First step: choosing a fitness function, four statistical indicators (RMSE, MSE, MAE, and RRSE) were applied as fitness functions (Eqs. 4, 5, 11, and 12). The evaluations indicated that the RMSE function provides the best results for predicting the X_{20}, $X_{50,}$ and X_{80} values.

$$\text{MSE} = \frac{1}{N}\sum_{i=1}^{N} \quad (X_{i-Predicted} - X_{i-Measured})^2 \quad (11)$$

$$\text{RRSE} = \sqrt{\frac{\sum_{i=1}^{N}\left(\text{Xi}_{pr} - \text{Xi}_{mes}\right)^2}{\sum_{i=1}^{N}\left(\bar{X}i_{mes} - \text{Xi}_{mes}\right)^2}} \quad (12)$$

Second step: assigning a set of terminals (blasthole diameter, powder factor, and blastability index from the terminals) and functions for generating the chromosomes according to the inputs and outputs parameters. The mathematical operators used as function in this study include + , - , * , / , x , x^2 , x^3 , x^(1/3) , 1/x , exp(x) , log(x) and sqrt.

Third step: determine the structure of chromosomes (including the number of chromosomes, genes, and the head size).

Fourth step: choosing the linking function. The multiplication function (+) was applied.

Fifth step: generating a set of genetic operators and rates. Based on the suggestions of the previous studies [5,41] and also trial and error the rate values were obtained.

Table 4 displays the parameters applied in the GEP model. Finally, the results of performance indicators according to considered fitness functions have been demonstrated in Table 5.

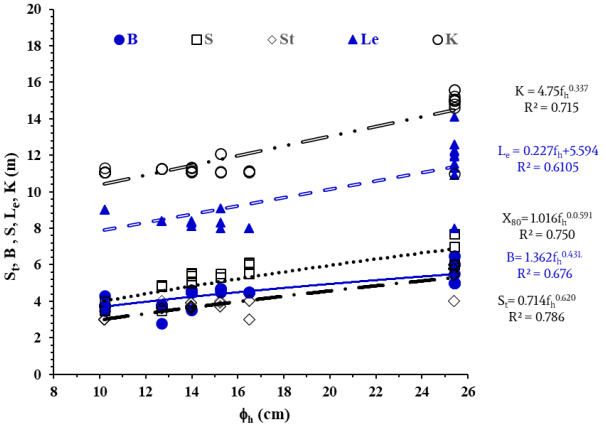

Figure 3. Relation between burden (B), spacing (S), stemming length (S_t), charge length (L_e), and bench height (K) with ϕ_h in blasting pattern of considered case studies.

Table 1. The rating of joint plane spacing in the calculation of the adjusted blastability index

Parameter	Description	Range (m)	Rate
Joint plane spacing (JPS)	Very close	<0.1	10
	Close	0.1 – 0.2	20
	Intermediate	0.2 – 0.5	30
	Wide	0.5 – 1	40
	Very wide	>1	50

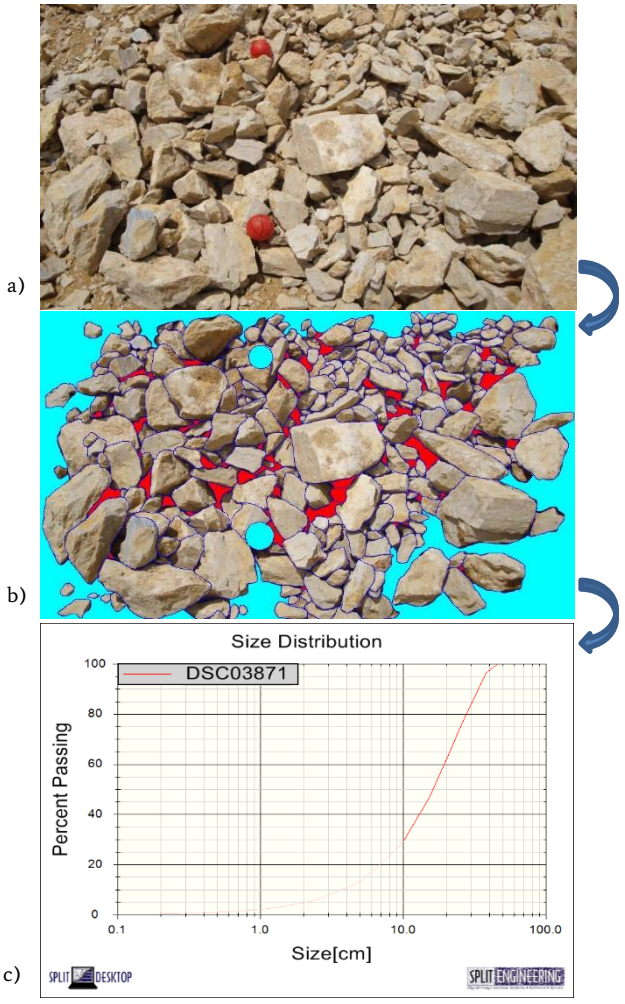

Figure 4. Digital image analysis process: a) Selection of an appropriate image of fermented rocks b) Fragments delineation with Split Desktop software c) determine the size distribution.

Table 2. Input and output parameters for performing GEP algorithm and MLR procedure.

Type	Parameter	Symbol	Unit	Min	Max	Std. Deviation
Input	Blasthole diameter	ϕ_h	mm	102.00	254.0	54.114
	Powder factor	q	kg/m³	0.38	1.723	0.339
	Blastability index	BI	-	32.58	84.250	12.496
Output	X_{20}	X_{20}	cm	4.00	14.300	2.508
	X_{50}	X_{50}	cm	10.40	32.100	5.242
	X_{80}	X_{80}	cm	16.80	64.200	12.080

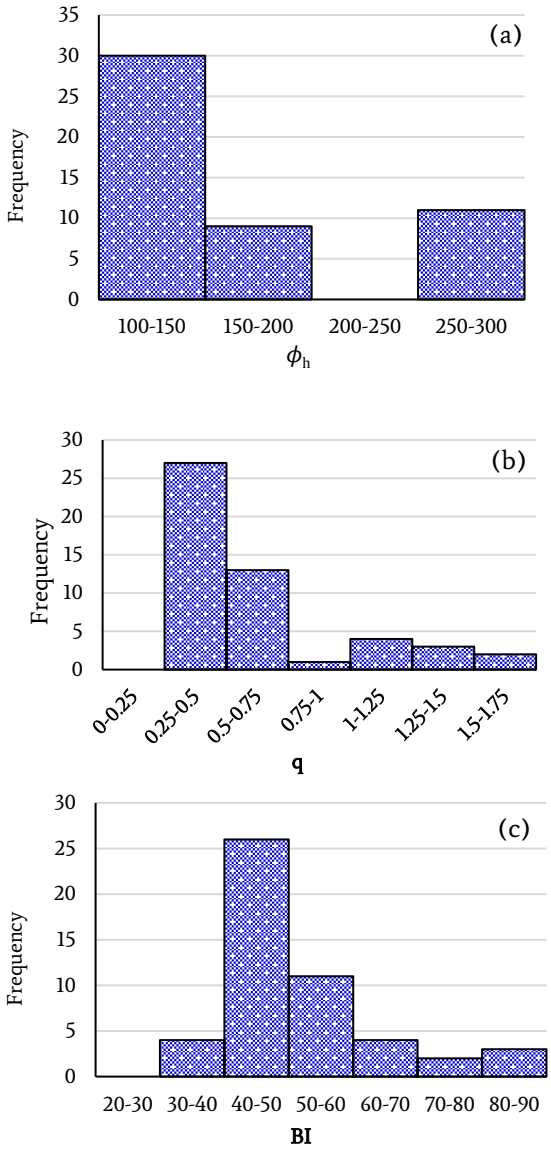

Figure 5. Frequency histograms of input parameters: a) Blasthole diameter, b) Powder factor, c) Blasability index (BI).

The best predicting models based on R^2, RMSE, MAE, and VAF are presented in Table 5. The model with high values for R^2 and VAF, and low values for RMSE and MAE confirms the high performance. Therefore, the best models for predicting X_{20}, X_{50}, and X_{80} are models with fitness functions of RMSE, MSE, and RMSE respectively according to obtained results. The training process was performed with 40 randomly selected data and 13 remaining data were used for testing the models. The values of statistical indicators for the prediction of X_{20}, X_{50}, and X_{80} with obtained GEP models are shown in Figure 6.

Table 3. The values of performance indicators for predicting X_{20}, X_{50}, and X_{80} by MLR.

	Train indicators				Test indicators			
Size	R^2	RMSE	MAE	VAF	R^2	RMSE	MAE	VAF
X_{20}	0.821	0.987	0.793	0.820	0.811	1.378	1.033	0.829
X_{50}	0.791	2.138	1.638	0.791	0.874	2.505	2.105	0.882
X_{80}	0.905	3.668	2.905	0.905	0.832	5.400	3.893	0.802

Table 4. Parameters of GEP model for prediction of X20, X50, and X80.

GEP Parameter	Value		
	Number of models		
	X_{20}	X_{50}	X_{80}
Fitness function	RMSE	RMSE	RMSE
Number of Genes	19	19	18
Head size	9	9	8
Mutation rate	0.001	0.001	0.001
Number of Chromosome	35	35	35
Number of genes	4	4	3
Gene recombination rate	0.003	0.003	0.003
Gene transportation rate	0.003	0.003	0.003
Number of generation	6000	6000	6000

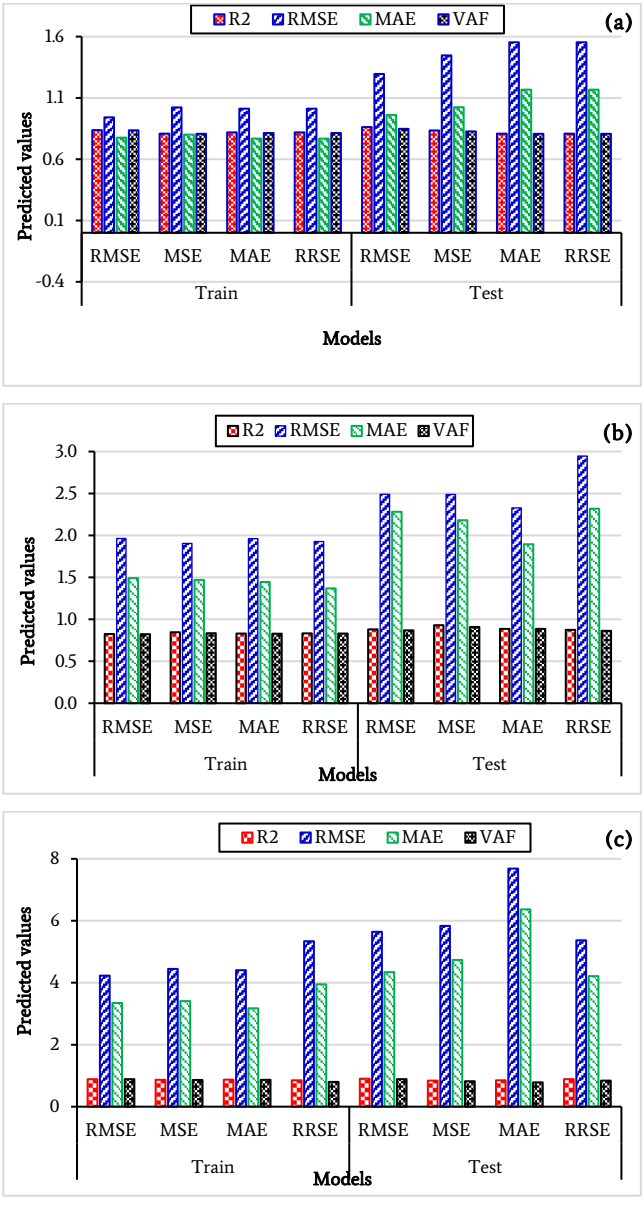

Figure 6. Amount of statistical indicators for predicting a) X_{20}, b) X_{50}, and c) X_{80} with GEP models.

Figure 7 shows the expression trees (ETs) of the obtained GEP models for prediction X_{20}, X_{50}, and X_{80} which are expressed based on input parameters and constant coefficients. Finally the Eqs. 12-14 are extracted from these expression trees and are proposed as the superlative predictors of the GEP model for the evaluation of rock fragmentation in this study.

$$X_{20} = \left(\sqrt[3]{(BI)^2 - \left(Exp(q)\right)^2}\right) + \left(\sqrt[3]{\left(Exp(\phi_h)\right) - \left(BI^2 + \sqrt[3]{q}\right)}\right) + (BI) + \left(\frac{q}{\left(Exp((q \times BI) + 0.77)\right) - \phi_h}\right) \quad (12)$$

$$X_{50} = (BI) + \left(Exp(-1.57)\right) + \left(\left(\left(\phi_h + (BI - 0.45)\right) - BI^3\right) \times \phi_h\right) + \left(\sqrt[3]{-3.29} \times \left(q - \frac{1}{(\phi_h \times (-8.06)) - 5.35}\right)\right) \quad (13)$$

$$X_{80} = \left(\left({\phi_h}^2 - \left((\phi_h \times q) \times {\phi_h}^3\right)\right)^2\right) + \left((2q - {\phi_h}^3) \times ((\phi_h - 0.73) - BI^2)\right) + (BI) \quad (14)$$

The statistical indicators (R^2, RMSE, VAF, and MAE) of the train and test results of optimized MLR and GEP models for prediction X_{20}, X_{50}, and X_{80} are shown in Figure 8.

The predicted X_{20}, X_{50}, and X_{80} as a function of considered parameters (ϕ_h, q and adjusted BI) using MLR and GEP models have been compared with the measured values of X_{20}, X_{50}, and X_{80} of 13 groups of test results in Figures. 9, 10, and 11 respectively.

According to the attained results in Figures. 9, 10, and 11, better correlations and performance of the achieved GEP models than MLR procedure models are concluded.

6. Sensitivity Analysis

sensitivity analysis was performed to identify the relative impact of each parameter on output in the mode using the cosine domain method [67]. All data pairs were utilized to construct a data array X as follows [67]:

$$X = \{x_1, x_2, x_3, ..., x_i, ..., x_n\} \quad (15)$$

Each of the elements, xi, in the data array X is a vector of lengths of m, that is:

$$X = \{x_1 1, x_2 2, x_3 3, ..., x_{im}\} \quad (16)$$

The strength of the relation between the dataset, xi, and xj, is presented as follows:

$$r_{ij} = \frac{\sum_{k=1}^{m} x_{ik} x_{jk}}{\sqrt{\sum_{k=1}^{m} x_{ik}^2 \sum_{k=1}^{m} x_{ik}^2}} \quad (17)$$

Figure 12 shows the strengths of the relations (rij values) between the model inputs and outputs. The results showed that, For the X20 and X80, the values of ϕ_h and BI have the greatest effect on the result, respectively. While for the X50, BI has the greatest effect on the output. Sensitivity analysis also showed that in all three outputs, q had the least effect.

7. Conclusions

A comprehensive study on rock fragmentation by blasting was performed for different zones in four open-pit mines. Blast pattern parameters including burden, spacing, stemming, charge length and bench height showed good correlations with ϕ_h. Thus, unlike the previous studies, these parallel parameters were ignored and rock fragmentation was investigated as a function of more effective and critical parameters of powder factor, blasthole diameter, and adjusted blastability index in the present study.

Table 5. Performance of the GEP models with considered fitness functions

	Methods	Train				Test			
		R^2	RMSE	MAE	VAF	R^2	RMSE	MAE	VAF
X_{20}	RMSE	0.837	0.942	0.776	0.837	0.862	1.295	0.962	0.848
	MSE	0.808	1.023	0.801	0.807	0.835	1.447	1.024	0.827
	MAE	0.819	1.012	0.768	0.814	0.808	1.553	1.167	0.807
	RRSE	0.819	1.012	0.768	0.814	0.808	1.553	1.167	0.807
X_{50}	RMSE	0.825	1.964	1.491	0.824	0.881	2.490	2.283	0.869
	MSE	0.846	1.905	1.469	0.834	0.929	2.488	2.182	0.910
	MAE	0.831	1.962	1.444	0.829	0.886	2.329	1.896	0.886
	RRSE	0.833	1.927	1.369	0.830	0.874	2.946	2.320	0.864
X_{80}	RMSE	0.888	4.231	3.348	0.886	0.904	5.644	4.346	0.889
	MSE	0.867	4.448	3.411	0.861	0.842	5.837	4.737	0.820
	MAE	0.871	4.406	3.177	0.868	0.850	7.687	6.368	0.785
	RRSE	0.853	5.341	3.949	0.799	0.885	5.370	4.213	0.840

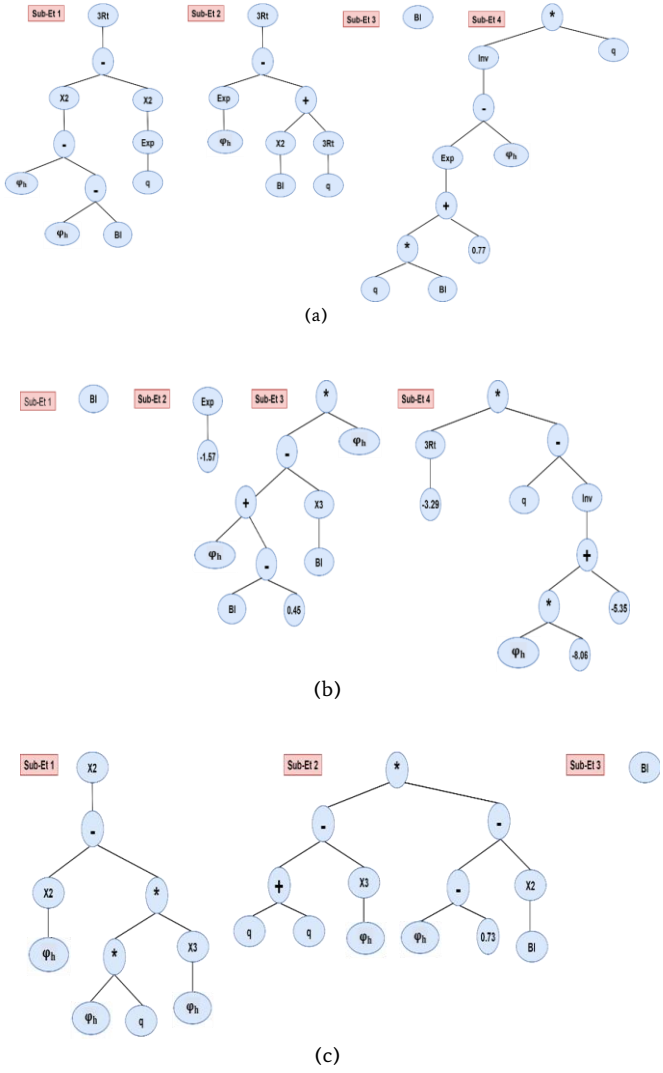

Figure 7. Expression trees of the GEP models for prediction a) X_{20}, b) X_{50}, and c) X_{80}.

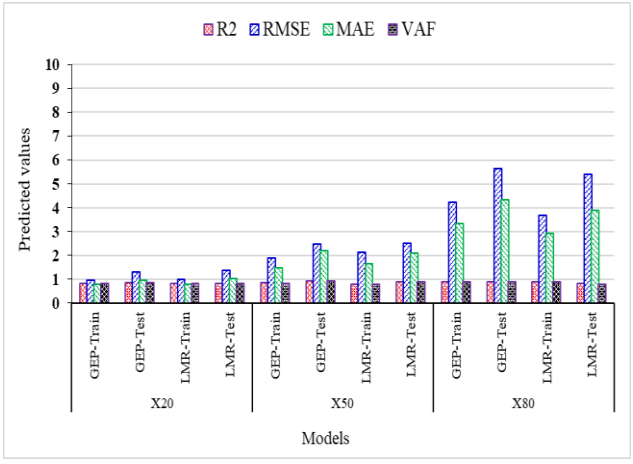

Figure 8. Comparison between performance indicators for MLR and GEP models.

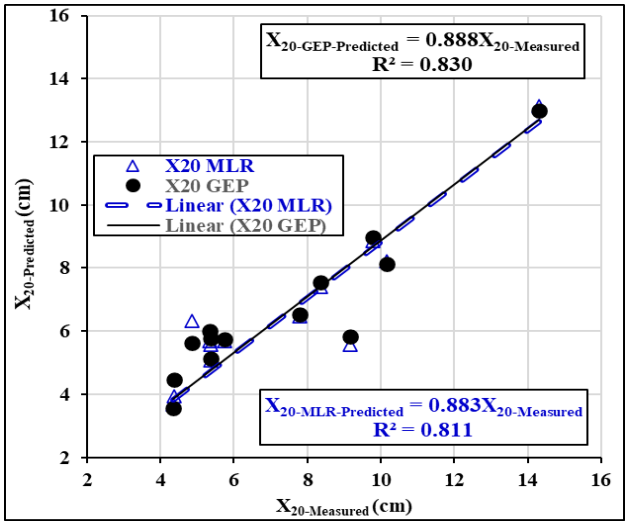

Figure 9. Comparison between predicted and measured X_{20} using MLR and GEP models.

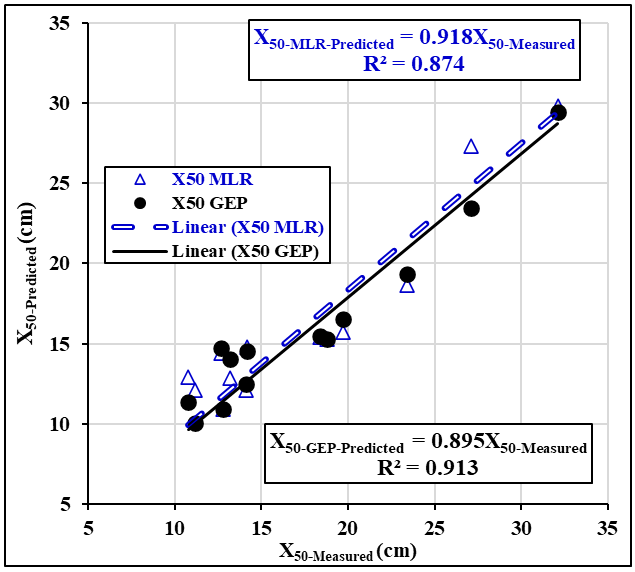

Figure 10. Comparison between predicted and predicted X_{50} using MLR and GEP models

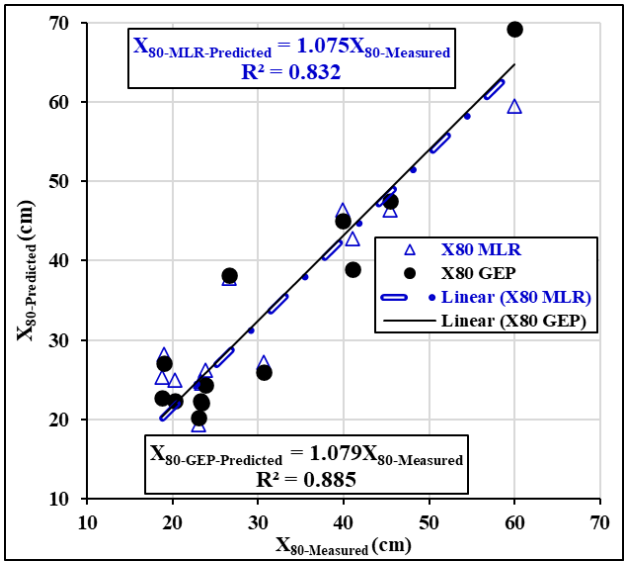

Figure 11. Comparison between predicted and measured X_{80S} using MLR and GEP models

The input and output data had a wide variation for different zones and new comprehensive models were developed to predict each fragment size including X_{20}, X_{50}, and X_{80} as a function of adjusted BI, ϕ_h, and q by GEP algorithm and MLR procedure using 53 datasets in several zones of Sungun open-pit copper mine, Rashakan limestone mine, Soufian limestone mine and Golgohar open-pit iron mine in Iran. A comparison of the considered statistical parameters (R^2, RMSE, MAE, and VAF) revealed the high ability of achieved GEP models to predict the size of fragmented rocks in blasting operations and provided the superiority of GEP over MLR models in this field. Finally, the sensitivity analysis showed that the values of input parameters ϕ_h and BI have more impact than the parameter of q on all three outputs.

8. Acknowledgments

The authors would like to acknowledge the managers and personnel of Sungun, Golgohar, Rashakan, and Soufian mines for their kind help and continuous support for this study.

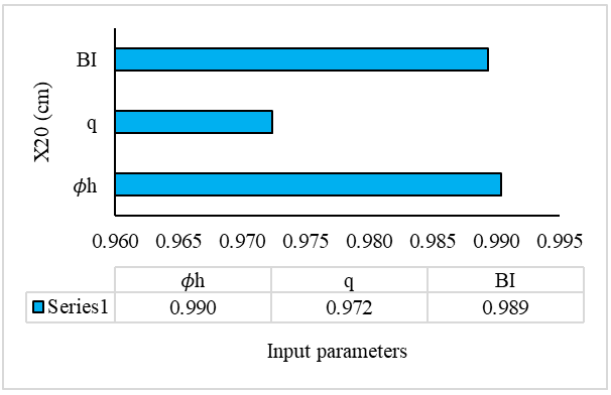

(a)

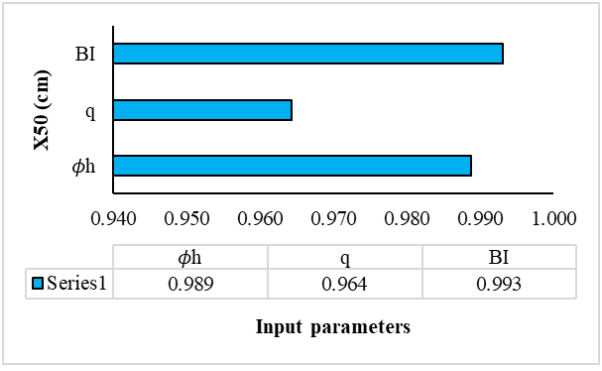

(b)

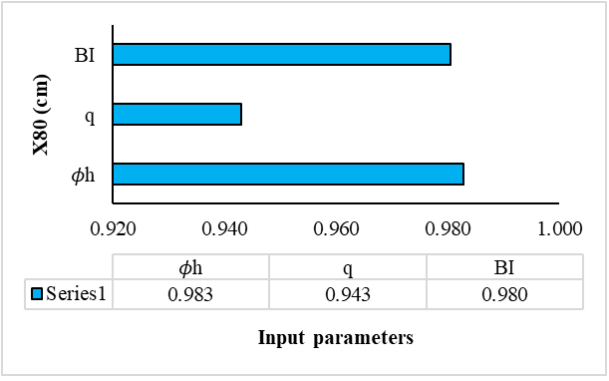

(c)

Figure 12. The impact of input parameters on outputs/

REFERENCES

[1] Jimeno, C.L., Jimeno, E.L. & Carcedo, F.J.A. (1995). Drilling and Blasting of Rocks. A.A.Balkema, Rotterdam.

[2] An, H.M., Liu, H.Y., Han, H., Zheng, X. &Wang, X. (2017). Hybrid finite-discrete element modelling of dynamic fracture and resultant fragment casting and muck-piling by rock blast. Computers and Geotechnics, 81,322-345. https://doi.org/10.1016/j.compgeo.2016.09.007.

[3] Sastry, V.R. (2016). Rock blasting technology: The way forward. Proceedings of the conference on Recent Advances in Rock Engineering (RARE 2016), 606 – 611. https://doi.org/10.2991/rare-16.2016.97.

[4] Faradonbeh, R. S., Armaghani, D. J., Amnieh, H. B., & Mohamad, E. T. (2018). Prediction and minimization of blast-induced flyrock using gene expression programming and firefly

algorithm. Neural Computing and Applications, 29(6), 269-281.

[5] Monjezi, M., Dehghani, H., Shakeri, J., & Mehrdanesh, A. (2021). Optimization of prediction of flyrock using linear multivariate regression (LMR) and gene expression programming (GEP)—Topal Novin mine, Iran. Arabian Journal of Geosciences, 14(15), 1-12.

[6] Faradonbeh, R.S. & Monjezi, M. (2017). Prediction and minimization of blast-induced ground vibration using two robust meta-heuristic algorithms. Engineering with Computers. 33, 835–851. https://doi.org/10.1007/s00366-017-0501-6.

[7] Hasanipanah, M., Faradonbeh, R.S., Amnieh, H.B. et al. (2017). Forecasting blast-induced ground vibration developing a CART model. Engineering with Computers 33, 307–316. https://doi.org/10.1007/s00366-016-0475-9

[8] Şenyur, M. G. (1998). A statistical analysis of fragmentation after single hole bench blasting. Rock Mechanics and Rock Engineering, 31(3), 181-196. https://doi.org/10.1007/s006030050018.

[9] Ozkahraman, H.T. (2006). Fragmentation assessment and design of blast pattern at Goltas Limestone Quarry, Turkey. International Journal of Rock Mechanics and Mining Sciences, 43(4), 628-633. https://doi.org/10.1016/j.ijrmms.2005.09.004.

[10] Kuznetsov, V.M. (1973). The mean diameter of the fragments formed by blasting rock. Journal of Mining Science, 9,144–148.

[11] Cunningham, C.V.B. (1983). The Kuz-Ram Model for Prediction of Fragmentation from Blasting. In: First International Symposium on Rock Fragmentation by Blasting, Luleå University of Technology, Lulea 2:439-453.

[12] Nourian, A. & Moomivand, H. (2020). Development of a new model to predict uniformity index of fragment size distribution based on the blasthole parameters and blastability index, Journal of Mining Science, 56(1),47–58. https://doi.org/10.1134/S1062739120016478.

[13] Monjezi, M., Amini khoshalan, H. & Yazdian, A. (2011). Optimization of Blast Parameters Using Genetic Algorithms. International Journal of Rock Mechanics and Mining Sciences, 48,864–869. https://doi.org/10.1007/s12517-010-0185-3.

[14] Mojtahedi, S.F.F., Ebtehaj, I., Hasanipanah, M., et al. (2019). Proposing a novel hybrid intelligent model for the simulation of particle size distribution resulting from blasting. Engineering with Computers, 35,47–56. https://doi.org/ 10.1007/s00366-018-0582-x.

[15] Zhang., S., Bui, X. N., Trung, N.T., Nguyen, H. & Bui, H.B. (2020). Prediction of rock size distribution in mine bench blasting using a novel ant colony optimization-based boosted regression tree technique. Natural Resources Research, 29(2), 867-886. https://doi.org/10.1007/s11053-019-09603-4.

[16] Akyildiz, O. & Hudaverdi, T. (2020). ANFIS modelling for blast fragmentation and blast-induced vibrations considering stiffness ratio. Arabian Journal of Geoscience, 13,1162. https://doi.org/10.1007/s12517-020-06189-7.

[17] Faramarzi, F., Mansouri, H. & Ebrahimi Farsangi, M.A. (2013). A Rock Engineering systems-based model to predict rock fragmentation by blasting. International Journal of Rock Mechanics and Mining Sciences, 60, 82–94. https://doi.org/10.1016/j.ijrmms.2012.12.045.

[18] Azadmehr, A., Jalali, S.M.E. & Pourrahimian, Y. (2019). An application of rock engineering system for assessment of the rock mass fragmentation: A hybrid approach and case study. Rock Mechanics and Rock Engineering, 52, 4403–4419. https://doi.org/10.1007/s00603-019-01848-y.

[19] Kulatilake, P.H.S.W., Qiong, W., Hudaverd, T. & Kuzu, C. (2010). Median particle size prediction in rock blast fragmentation using neural networks. Engineering Geology, 114:298–311.

[20] Moomivand, H. & Vandyousefi, H. (2020). Development of a new empirical fragmentation model using rock mass properties, blasthole parameters, and powder factor. Arabian Journal of Geoscience, 13, 1173. https://doi.org/10.1007/s12517- 20-06110-2.

[21] Monjezi, M., Amiri H., Farrokhi, A. & Goshtasbi, K. (2010). Prediction of rock fragmentation due to blasting in Sarcheshmeh copper mine using artificial neural networks. Geotechnical and Geological Engineering, 28(4), 423-430. https://doi.org/10.1007/s10706-010-9302-z.

[22] Amini, H., Gholami, R., Monjezi, M., Torabi, S.R. & Zadhesh, J. (2011). Evaluation of flyrock phenomenon due to blasting operation by Support Vector Machine. Neural Computing and Applications, 21, 2077-2085. https://doi.org/10.1007/S00521-011-0631-5.

[23] Karami A. & Afiuni-Zadeh, S. (2013). Sizing of rock fragmentation modeling due to bench blasting using adaptive neuro-fuzzy inference system (ANFIS). International Journal of Mining Science and Technology, 23 (6), 809-813. https://doi.org/10.1016/ j.ijmst. 2013.10.005.

[24] Monjezi, M., Mohamadi, H.A., Barati, B. & Khandelwal, M. (2014). Application of soft computing in predicting rock fragmentation to reduce environmental blasting side effects. Arabian Journal of Geoscience, 7(2), 505-511. https://doi.org/10.1007/s12517-012-0770-8.

[25] Shams, S., Monjezi, M., Majd, V.J., et al. (2015). Application of fuzzy inference system for prediction of rock fragmentation induced by blasting. Arabian Journal of Geosciences, 8,10819–10832. https://doi.org/10.1007/s12517-015-1952-y.

[26] Gao, W., Karbasi, M., Hasanipanah, M. & Zhang Guo, J. (2018). Developing GPR model for forecasting the rock fragmentation in surface mines. Engineering with Computers, 34(2), 339-345.

[27] Mehrdanesh, A., Monjezi, M. & Sayadi, A.R. (2018). Evaluation of effect of rock mass properties on fragmentation using robust techniques. Engineering with Computers, 253–260.

[28] Hasanipanah, M., Amnieh, H.B., Arab, H. & Zamzam, M.S. (2018). Feasibility of PSO–ANFIS model to estimate rock fragmentation produced by mine blasting. Neural Computing and Applications, 30(4), 1015-1024. https://doi.org/ 10.1007/s00521-016-2746-1.

[29] Fang, Q., Nguyen, H., Bui, X.N., Nguyen-Thoi, T. & Zhou, J. (2021). Modeling of rock fragmentation by firefly optimization algorithm and boosted generalized additive model. Neural Computing and Applications, 33, 3503–3519.

[30] Shirani Faradonbeh, R., Taheri, A. & Karakus, M. (2022). The propensity of the over-stressed rock masses to different failure mechanisms based on a hybrid probabilistic approach, Tunnelling and Underground Space Technology, 119, https://doi.org/10.1016/j.tust.2021.104214.

[31] Shirani Faradonbeh, R., Shaffiee Haghshenas, S., Taheri, A. et al. Application of self-organizing map and fuzzy c-mean techniques for rockburst clustering in deep underground projects. Neural Comput & Applic 32, 8545–8559 (2020). https://doi.org/10.1007/s00521-019-04353-z

[32] Shakeri, J., Amini Khoshalan, H., Dehghani, H., Onyelowe, K., Bascompta, M. (2022). Developing new models for flyrock distance assessment in open-pit mines. Journal of Mining and

Environment, -. doi: 10.22044/jme.2022.11805.2170

[33] Shirani Faradonbeh, R., Taheri, A., Ribeiro e Sousa, L. & Karakus, M. (2020). Rockburst assessment in deep geotechnical conditions using true-triaxial tests and data-driven approaches, International Journal of Rock Mechanics and Mining Sciences,128: 104279, https://doi.org/10.1016/j.ijrmms.2020.104279.

[34] Shaffiee Haghshenas, S., Shirani Faradonbeh, R., Mikaeil, R., et al. (2019). A new conventional criterion for the performance evaluation of gang saw machines, Measurement, 146: 159-170, https://doi.org/10.1016/j.measurement.2019.06.031.

[35] Shirani Faradonbeh, R., Taheri, A. & Karakus, M. (2022). Fatigue Failure Characteristics of Sandstone Under Different Confining Pressures. Rock Mechanics Rock Engineering, 55, 1227–1252 https://doi.org/10.1007/s00603-021-02726-2

[36] Monjezi, M., Rezaei, M. & Yazdian Varjani, A. (2009). Prediction of Rock Fragmentation due to Blasting in Gol-E-Gohar Iron Mine Using Fuzzy Logic. International Journal of Rock Mechanics and Mining Sciences, 46 (8), 1273–1280. https://doi.org/10.1016/j.ijrmms.2009.05.005.

[37] Ebrahimi, E., Monjezi, M., Khalesi, M.R. & Jahed Armaghani, D. (2016). Prediction and optimization of back-break and rock fragmentation using an artificial neural network and a bee colony algorithm. Bulletin of Engineering Geology and the Environment, 75(1), 27-36.

[38] Faraji Asl, P., Monjezi, M., Hamidi, J.K. et al. (2018). Optimization of flyrock and rock fragmentation in the Tajareh limestone mine using metaheuristics method of firefly algorithm. Engineering with Computers, 34, 241–251. https://doi.org/10.1007/s00366-017-0535-9.

[39] Huang, J., Asteris, P.G., Pasha, S.M.K., Mohammed, A.S. & Hasanipanah, M. (2020). A new auto-tuning model for predicting the rock fragmentation: a cat swarm optimization algorithm. Engineering with Computers. https://doi.org/10.1007/s00366-020-01207-4.

[40] Montgomery, D.C. & Peck, E.A. (1992). Introduction to Linear Regression Analysis. Wiley, New York, USA.

[41] Shakeri, J., Shokri, B.J. & Dehghani, H. (2020). Prediction of blast-induced ground vibration using gene expression programming (GEP), artificial neural networks (ANNS), and linear multivariate regression (MLR). Archives of Mining Sciences, 65(2), 317-335. https://doi.org/10.24425/ams.2020.133195.

[42]. Onyelowe, K. C., Shakeri, J., Amini-Khoshalan, H., Usungedo, T. F., & Alimoradi-Jazi, M. (2022). Computational Modeling of Desiccation Properties (CW, LS, and VS) of Waste-Based Activated Ash-Treated Black Cotton Soil for Sustainable Subgrade Using Artificial Neural Network, Gray-Wolf, and Moth-Flame Optimization Techniques. Advances in Materials Science and Engineering. doi: 10.1155/2022/4602064.

[43] Rosin P., Rammler, E. (1933). The laws governing the fineness of powdered coal, Journal of the Institute of Fuel, 7: 29–36.

[44] Onyelowe, K. C., Shakeri, J., Amini-Khoshalann, H., Salahudeen, A. B., Arinze, E. E., & Ugwu, H. U. (2021). Application of ANFIS hybrids to predict coefficients of curvature and uniformity of treated unsaturated lateritic soil for sustainable earthworks. Cleaner Materials, 1, 100005.

[45] Abyaneh, H.Z. (2014). Evaluation of multivariate linear regression and artificial neural networks in prediction of water quality parameters. Journal of Environmental Health Science and Engineering, 12(1), 40. https://doi.org/10.1186/2052-336X-12-40.

[46] Ferreira, C. (2006). Gene expression programming: mathematical modeling by artificial intelligence. 21, Springer.

[47] Majidifard, H., Jahangiri, B., Buttlar, W.G. & Alavi, A.H. (2019). New machine learning-based prediction models for fracture energy of asphalt mixtures. Measurement, 135, 438-451. https://doi.org/10.1016/j. measurement. 2018.11.081.

[48] Mahdiyar, A., Jahed Armaghani, D., Koopialipoor, M., Hedayat, A., Abdullah, A. & Yahya, K. (2020). Practical Risk Assessment of Ground Vibrations Resulting from Blasting Using Gene Expression Programming and Monte Carlo Simulation Techniques. Applied Sciences, 10, 472.

[49] Bolandi, H., Banzhaf, W., Lajnef, N., Barri, K. & Alavi, A.H. (2019). Bond strength prediction of FRP-bar reinforced concrete: a multi-gene genetic programming approach. In Proceedings of the Genetic and Evolutionary Computation Conference Companion, 364-36.

[50] Baykasoğlu, A., Güllü, H., Çanakçi, H. & Özbakir, L., (2008). Prediction of compressive and tensile strength of limestone via genetic programming. Expert Systems with Applications, 35(1-2), 111-123. https://doi.org/10.1016/j. eswa.2007.06.006.

[51] Faradonbeh RS, Jahed Armaghani D, Monjezi M & Mohamad ET. (2016). Genetic programming and gene expression programming for flyrock assessment due to mine blasting. International Journal of Rock Mechanics and Mining Sciences, 88, 254-264. https://doi.org/10.1016/j.ijrmms.2016.07.028.

[52]. Amini Khoshalan, H., Shakeri, J., Najmoddini, I., Asadizadeh, M. (2021). Forecasting copper price by application of robust artificial intelligence techniques, Resources Policy, 73, 102239.

[53]. Onyelowe, K. C., & Shakeri, J. (2021). Intelligent prediction of coefficients of curvature and uniformity of hybrid cement modified unsaturated soil with NQF inclusion. Cleaner Engineering and Technology, 4, 100152.

[54] Ramesh, A., Hajihassani, M. & Rashiddel, A. (2020). Ground movements prediction in shield-driven tunnels using gene expression programming. Open Construction and Building Technology Journal, 14(1), 286-297. https://doi.org/10.2174/1874836802014010286.

[55] Mollahasani, A., Alavi, A.H. & Gandomi, A.H. (2011). Empirical modeling of plate load test moduli of soil via gene expression programming. Computers and Geotechnics, 38(2), 281-286. https://doi.org/10.1016/j. compgeo. 2010. 11 .008.

[56] Dindarloo, S.R, Prediction of blast-induced ground vibrations via genetic programming. International Journal of Mining Science and Technology, 2015, 25(6), 1011-1015. https://doi.org/10.1016/j.ijmst.2015.09.020.

[57] Jahed Armaghani, D., Safari, V., Fahimifar, A., Monjezi, M. & Mohammadi., M.A. (2018). Uniaxial compressive strength prediction through a new technique based on gene expression programming. Neural Computing and Applications, 30(11), 3523-3532. https://doi.org/10.1007/s00521-017-2939-2.

[58] Ferreira, C. (2001). Gene expression programming: a new adaptive algorithm for solving problems. arxiv preprint cs/0102027.

[59] Faradonbeh, R.S., Armaghani, D.J., Monjezi, M. & Mohamad, E.T. (2016). Genetic programming and gene expression programming for flyrock assessment due to mine blasting. International Journal of Rock Mechanics and Mining Sciences, 88, 254-264. https://doi.org/10.1016/j.ijrmms.2016.07.028.

[60] Lilly, P.A. (1986). An empirical method of assessing rock mass

blastability. In: Proceedings of the large open-pit planning conference. Australian IMM, Parkville, Victoria, 89–92

[61] Lilly, P.A. (1992). The use of the Blastability Index in the design of blasts for open-pit mines. Western Australian Conference on Mining Geotechnics, Kalgoorlie, 421–426.

[62] Split Engineering LLC Team, (2015). Manual of split desktop image analysis software, Version 3.1. P.O. Box 41766, Tucson, AZ 85717–1766, http://www.spliteng.com.

[63] Masoumi Nasab, S.M., Jalali, S.E. & Noroozi, M. (2019). Performance comparison of commercial software tools to determine size distribution of fragmented rocks. Journal of Mineral Resources Engineering, 4(3), 61 – 65. https://doi.org/10.30479/ JMRE.2019.8892.1136.

[64] Azizi, A. & Moomivand, H. (2021). A New Approach to Represent Impact of Discontinuity Spacing and Rock Mass Description on the Median Fragment Size of Blasted Rocks Using Image Analysis of Rock Mass. Rock Mechanics and Rock Engineering, 4, 1-26. https://doi.org/10.1007/s00603-020-02360-4.

[65] Shakeri, J., Asadizadeh, M., & Babanouri, N. (2022). The prediction of dynamic energy behavior of a Brazilian disk containing nonpersistent joints subjected to drop hammer test utilizing heuristic approaches. Neural Computing and Applications, 1-16.

[66] Onyelowe, K. C., Mahesh, C. B., Srikanth, B., Nwa-David, C., Obimba-Wogu, J., & Shakeri, J. (2021). Support vector machine (SVM) prediction of coefficients of curvature and uniformity of hybrid cement modified unsaturated soil with NQF inclusion. Cleaner Engineering and Technology, 5, 100290.

[67] Yang, Y., & Zhang, Q. (1997). A hierarchical analysis for rock engineering using artificial neural networks. Rock Mechanics and Rock Engineering, 30(4), 207-222.